Solid State Science and Technology, Vol. 24, No 2 (2016) 189-196
ISSN 0128-7389 | *http://journal.masshp.net*

EFFECT OF RARE-EARTH DOPING ON STRUCTURAL, ELECTRONIC AND OPTICAL PROPERTIES OF PEROVSKITE $PbTiO_3$: FIRST PRINCIPLES APPROACH

N.H. Hussin[1,2], M.N.S. Saimin[1,2] ,N. Salleh[2], O.H. Hassan[3,5], M.Z.A. Yahya[4, 5] and M.F.M. Taib[1, 5]

[1]*Faculty of Applied Sciences, Universiti Teknologi MARA 40450 Shah Alam,Selangor Malaysia*

[2]*Faculty of Applied Sciences, Universiti Teknologi MARA 35400 Tapah,Perak, Malaysia*

[3]*Department of Industrial Ceramics, Faculty of Arts & Design, Universiti Teknologi MARA, 40450 Shah Alam,Selangor Malaysia*

[4]*Department of Defence Science, Universiti Pertahanan Nasional Malaysia, 57000 Kuala Lumpur, Malaysia*

[5]*Ionic Materials and Devices (iMADE) Research Laboratory, Institute of Science, Universiti Teknologi MARA, 40450 Shah Alam, Selangor, Malaysia*

Corresponding author: mfariz@salam.uitm.edu.my

ABSTRACT

The structural, electronic and optical properties of rare-earth (La and Sm) doped ferroelectric $PbTiO_3$ (tetragonal, P4mm space group) are investigated via first principles study. The calculations were performed using local density approximation (LDA) and generalized gradient approximation (GGA) functional as implemented in Cambridge Serial Total Energy Package (CASTEP) computer code. The effect of rare-earth doping change the structural properties of $PbTiO_3$. The rare-earth doping in $PbTiO_3$ reduce its band gap and the density of states (DOS) present the chemical bonding that formed in the doped materials. Refractive index and dielectric constant of the doped-$PbTiO_3$ increase. The results are compared with experimental and other theoretical data.

INTRODUCTION

Lead titanate is a typical perovskite compound and it has been used for infrared sensors, electromechanical transducers and optical modulators as its large dielectric constant, and noticeable pyroelectric, piezoelectric and electro-optic effects [1]–[3]. The structure of the perfect $PbTiO_3$ has a cubic symmetry [4] and also known as paraelectric. Its lattice consists of a corner-sharing oxygen octahedral with interpenetrating simple cubic lattices of Pb and Ti cations [5]. The Ti cations sit at the center of each one of the oxygen octahedrals, while the Pb ions lie in 12-fold coordinated sites between the

octahedral. The properties of $PbTiO_3$ can be easily modified[6], for example, the Pb, Ti, O atoms can be replaced by other impurity atoms. $PbTiO_3$ has been studied extensively. Biedrzycki et al. observed the electron emission of Ca-doped $PbTiO_3$ semiconducting thin films. Jaber et al. prepared La-doped $PbTiO_3$ thin films and studied the composition of the films [7]. Palkar et al. investigated Si-doped $PbTiO_3$ to understand the effect of Si on the ferroelectric characteristics. Hovsepyan et al. reported the far-infrared reflectivity spectra and electronic properties of the zirconium and copper doped $PbTiO_3$ single-crystal films. However, the conductivity and photocatalytic property of element doping $PbTiO_3$ have not been studied further. As we know, N replacing O in most compounds shows p-type conductivity. Furthermore, the La and Sm dopants lead to the band gap narrowing in the crystals [8]. In this paper, we studied the electronic structures and optical properties of intrinsic $PbTiO_3$ and with rare earth La and Sm doped $PbTiO_3$ based on the first-principles calculations. Theoretical computation studies based on ab initio calculations can yield important information regarding the electrical and structural properties of these solids. Moreover, the theoretic study would also predict the special properties induced by La and Sm dopants. The work would be helpful for designing experiments and explaining the phenomenon in experimental study.

EXPERIMENTAL

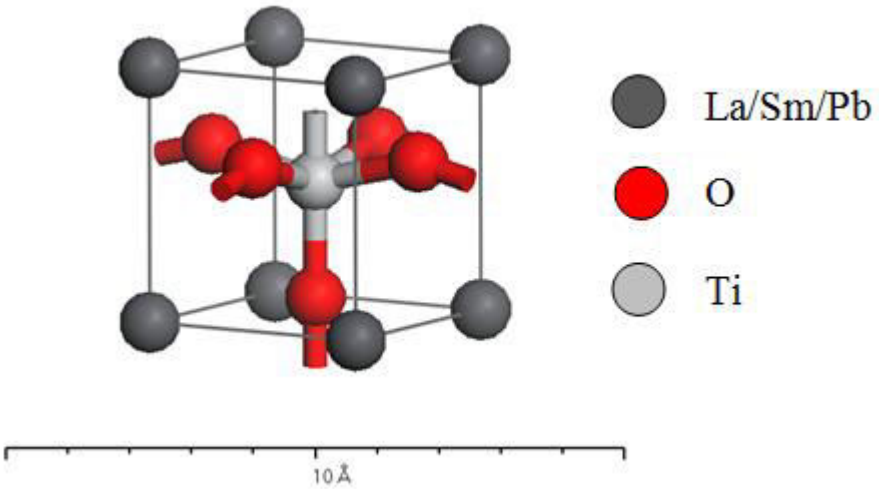

Figure 1: The crystal structure of La and Sm doped $PbTiO_3$ with tetragonal structure (P4mm phase group)

Structural, electronic and optical properties of tetragonal $PbLaTiO_3$ and $PbSmTiO_3$ material with P4mm phases are performed using first principles method based on density functional theory (DFT) implemented in Cambridge Serial Total Energy Package plane wave code [9] computer code.. Generalized gradient approximation (GGA) within the Perdew–Burke–Ernzerhoffor solid (PBEsol) [14] is used to describe the exchange and correlation potential. This functional has already been successfully employed in studies of structural, electronic and optical properties of the $PbLaTiO_3$ and $PbSmTiO_3$. A plane-wave cut off energy with 340 eV is applied. We use ultrasoft pseudopotentials, a plane-wave basis set, and a conjugate-gradients algorithm to

compute total energies and forces for a variety of crystal configurations. The method and the details of the pseudopotentials employed have been described elsewhere. The Brillouin Zone with the 6x6x6 k-point (customized) is sampled. In this work, the focus is on the tetragonal structure (space group P4mm) structure. A stress threshold of 0.05 GPa is used for cell relaxation, and forces on ions are converged below 0.03 eV/Å.

RESULTS AND DISCUSSION

Structural properties of Sm and La doped $PbTiO_3$

Table 1: Calculated structural parameter (lattice constant (*a* and *c* in Å), atomic distance, volume (V in $Å^3$) and total energy (E in eV) of tetragonal $PbLaTiO_3$ with P4mm space group

	Functionals			**Experiment** [13]
	LDA	**GGA PBE**	**GGA PBEsol**	
Lattice Parameter (Å)				
a	3.911 **(-2.11%)**	3.992 **(4.23%)**	3.947 **(3.05%)**	3.83
c	3.910 **(-2.74%)**	4.015 **(-0.12%)**	3.950 **(-1.74%)**	4.02
c/a	0.990	1.005	1.000	1.050
Volume ($Å^3$)	59.819	63.979	61.519	58.969
Total Energy (eV)	-8367.39	-8362.76	-8348.02	

The value of unit cell lattice parameter, volume and total energy of tetragonal (P4mm space group) of $PbLaTiO_3$ and $PbSmTiO_3$ after optimized from the geometry optimization calculation are listed in Table 1. Structural optimizations of $PbLaTiO_3$ and tetragonal using different exchange correlations LDA-CAPZ, GGA-PBE, and GGA-PBEsol as shown in Table 1. The result of obtained for $PbLaTiO_3$ by using LDA-CAPZ in this work was underestimated, compared with GGA-PBE and GGA-PBEsol. For the $PbSmTiO_3$ the GGA-PBE are closed to the experimental data for Sm doped $PbTiO_3$ and this result obtained by CASTEP computer code was in the good agreement by a recent study of $PbTiO_3$. In addition, our calculation on the lattice parameter, *a* of tetragonal $PbLaTiO_3$ shows that functional LDA-CAPZ is more accurate with percentage difference of -2.11% compared with GGA-PBE and GGA-PBEsol which is 4.23% and 3.05% respectively. While for tetragonal $PbSmTiO_3$ the GGA-PBE show the accurateness of the lattice calculation which is 0.49% compared with LDA-CAPZ and GGA-PBEsol which is -1.57% and 0.63% respectively. Both of the lattice parameter for $PbLaTiO_3$ and $PbSmTiO_3$ are compared with experimental data since the computational

calculation can give the best method to support the experiment data in constant parameter. The lattice variation will give the significant factor of the material constancy and the other calculation of properties in perovskite oxide. Therefore, we should ensure that the structural calculation used is acceptable, although there is the lack study of $PbLaTiO_3$ using first principles method. The present work also shows that the tetragonality of $PbLaTiO_3$ also were compared with different functional. The functional LDA-CAPZ and GGA-PBE show that higher tetragonality which for both materials compared with GGA-PBEsol as listed in table 1 and table 2. The tetragonality of material very impotant in analyzing the spontaneous polarization.

Table 2.: Calculated structural parameter (lattice constant (*a* and *c* in Å), atomic distance, volume (V in $Å^3$) and total energy (E in eV) of tetragonal $PbSmTiO_3$ with P4mm space group

	Functionals			**Experiment** [15]
	LDA	**GGA PBE**	**GGA PBEsol**	
Lattice Parameter (Å)				
a	3.859 **(-1.57%)**	3.940 **(0.49%)**	3.896 **(0.63%)**	3.9207
c	3.868 **(-4.93%)**	3.956 **(-2.40%)**	3.906 **(-3.99%)**	4.0684
c/a	1.002	1.004	1.003	1.0376
Volume ($Å^3$)	57.581	61.412	59.300	62.53
Total Energy (eV)	-9704.15	-9705.09	-9689.27	

Band gap and density of states (DOS) of PlaZT

The calculated electronic band structures along the direction G-F-Q-Z-G at the high-symmetry Brillouin zone of $PbLaTiO_3$ and $PbSmTiO_3$ tetragonal are shown in Figs. 2, respectively. The highest valence band (VB), which lies at the Fermi level (E_F) at 0 eV, is dominated by the O 2p at Q point. Meanwhile, the conduction band (CB) of $PbLaTiO_3$ and $PbSmTiO_3$ occurs at G point, which is primarily dominated by Ti 3d mixed at Pb and La p-state. The calculation of the electronic band gap shows that $PbLaTiO_3$ and $PbSmTiO_3$ has an indirect band gap with the highest value of 2.91 eV at Q-G. However, calculation of the band gap value of $PbLaTiO_3$ in this work is higher than $PbLaTiO_3$ as reported by [14]. The band gap value of $PbSmTiO_3$ also acceptable with other calculations. The values in present work in good agreement with other computational studies that reported values of tetragonal $PbLaTiO_3$ and $PbSmTiO_3$ with 2.9 eV and 2.4 eV with GGA calculation. Therefore, the exact and approximate value of $PbLaTiO_3$ and $PbSmTiO_3$ are needed to predict the experimental value of the band gap for single-phase $PbLaTiO_3$ and $PbSmTiO_3$.

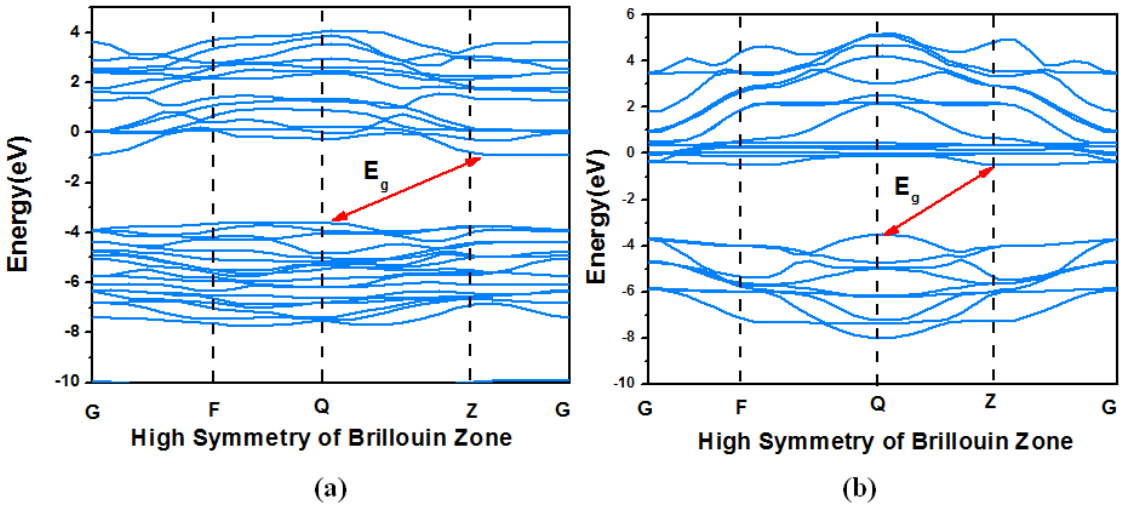

Figure 2: The calculated Band Gap of (a) $PbLaTiO_3$ and (b) $PbSmTiO_3$ along the high-symmetry Brillouin zone

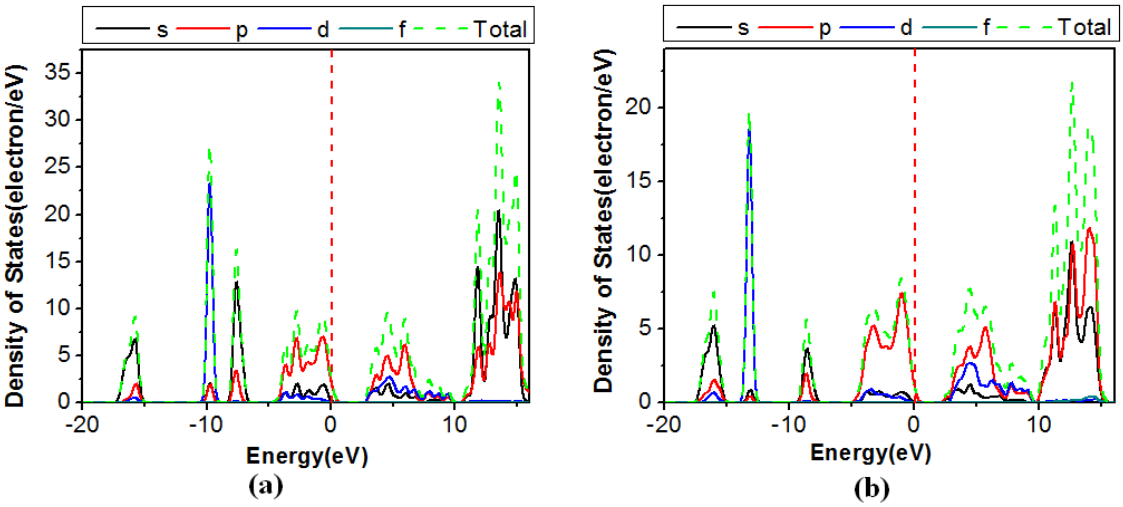

Figure 3: The Partial density of states (PDOS) of (a) $PbLaTiO_3$ and (b) $PbSmTiO_3$

The total and partial DOS for tetragonal $PbLaTiO_3$ and $PbSmTiO_3$ are shown in Fig. 3 below. The $PbLaTiO_3$ and $PbSmTiO_3$ reports in this work are similar with the report using first principles study. The highest VBs of the $PbLaTiO_3$ are mainly dominated by electron O 2p and the lowest CBs mainly originate from the Ti 3d and La 6p states. For the $PbSmTiO_3$ the VB also dominated by O 2p at the highest point and Sm 6p for the lowest CB. The $PbLaTiO_3$ and $PbSmTiO_3$ is a good ferroelectric material due to the special hybridization between special lone pair Pb 6s and O 2p at VB as shown in Figure 2. The separation between VBs and CBs for $PbLaTiO_3$ and $PbSmTiO_3$ is 2.91 eV and 2.82 eV as mentioned above. This is due to the different strength covalency of the Pb-O, Ti-O, La-O, Sm-O and Zr-O. The density of states calculations showed that the CB of $PbLaTiO_3$ and $PbSmTiO_3$ is shifted near to the fermi level of its band gap. This is

happen due to the dependent on extra electron or hole, change exchange potential between carriers. As a result, chemical potential of system changes and the Fermi level moves toward conduction or valence bands.

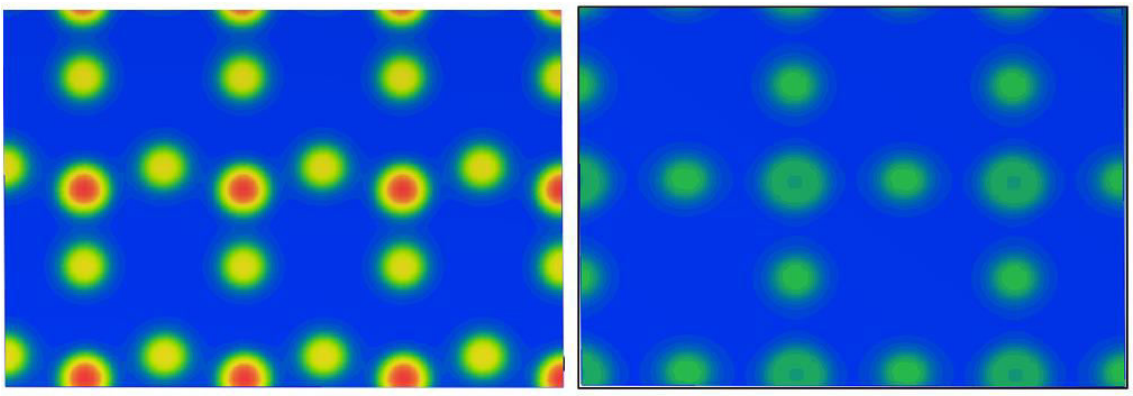

Figure 4: The calculated chemical bonding of (a) $PbLaTiO_3$ and (b) $PbSmTiO_3$

Figure 4 showed the chemical bonding that exist from $PbLaTiO_3$ and $PbSmTiO_3$. This results indicated the type of bonding that form in both materials with different dopant. To visualize the nature of the bond character and to explain the charge transfer and the bonding properties of our perovskite oxide $PbLaTiO_3$ and $PbSmTiO_3$, we examined charge density of this materials. For more detailed results, we used GGA-PBEsol ferroelectric phase. Fig. 4(a) and Fig. 4(b) show the charge densities for $PbLaTiO_3$ and $PbSmTiO_3$ GGA-PBEsol respectively. There are partial ionic and partial covalent bonds connecting Sm–O and La–O atoms. The Sm–O bonding is covalent with a weak degree of ionicity, whereas this covalence is due essentially to the hybridization effect of the La(d)/Sm(d) states and the O(p) states. Whereas La–O presented an ionic character with a weak covalence due to the weak interaction between the La (d) and the O (p) orbitals. The Sm-O also present the same bonding character as La-O. This nature of bonding is very clear in the GGA-PBEsol figures than in the GGA because the this functional treats the d and f states with efficiency and more exactly than other approximations.

Optical properties

Optical properties are closely related to the electronic band structure and phonon dispersion. Both types of interband optical transitions direct band gap and indirect band gap can be calculated from the first principles approach. In general, the optical properties can be explained in detail through knowledge of the complex dielectric function. The graph of real and imaginary part of dielectric function against energy from 0 eV to 40 eV that showed in the fig 4. The real part is for dielectric constant of this materials while imaginary part is for optical transition that exist in the conduction and valence bands due to the atomic hybridization. The dielectric constant for $PbLaTiO_3$ is 6.82 and for $PbSmTiO_3$ is 8.93. From the imaginary part of $PbLaTiO_3$ the

peaks are observed are 4 peaks which is 0.9, 8.7, 1.3 and 1.1. While for $PbSmTiO_3$ the imaginary part also showed the 4 peaks which is 2.9, 9.0, 0.6 and 1.0. The highest peaks that existed are related with electron transitions from O 2p states to the La 6p and Sm 6p states. From this dielectric function of $PbSmTiO_3$ give the higher value compared with $PbLaTiO_3$.

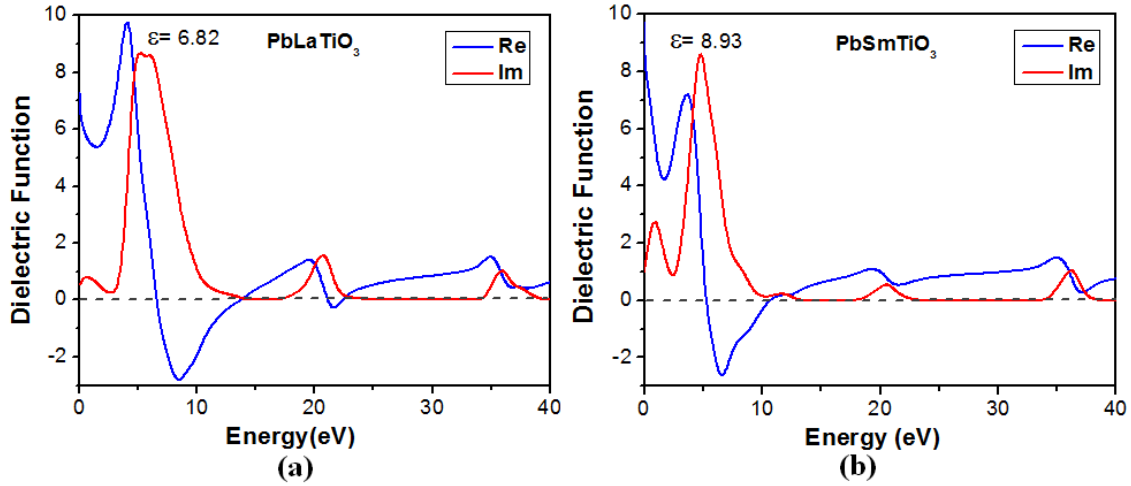

Figure 4: The calculated dielectric function of (a) $PbLaTiO_3$ and (b) $PbSmTiO_3$

The refractive indices (n) and the extinction coefficient (k) are calculated as shown in Figs 5 for $PbLaTiO_3$ and $PbSmTiO_3$**.** The values of static refractive index n (ω) are represented for PbLaTiO3 and PbSmTiO3 are increases with photon energy in the transparency region, peaking at 13 eV and 10 eV (ultraviolet region) as illustrated in Figs. 5 respectively. Subsequently, the value of n of PbLaTiO3 and PbSmTiO3 are 2.61 and 2.89 respectively and it is decreases with increase in photon energy to a minimum value. The intercept between refractive indices n and the extinction coefficient k of compound in this work correspond to the zero value for the real part of the dielectric function. The highest value of n can contribute to the efficient light scattering of materials such as in optical devices.

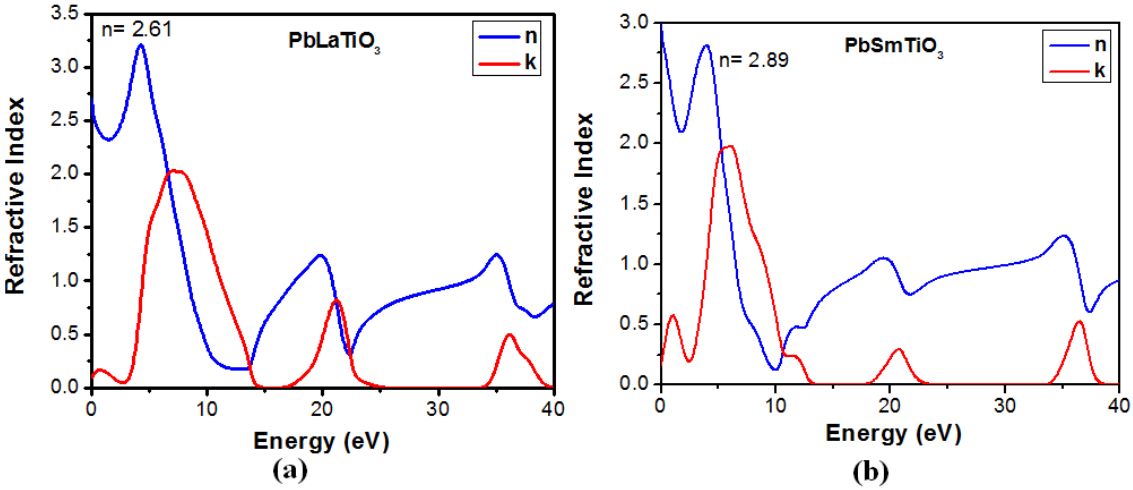

Figure 5: The calculated refractive index of (a) $PbLaTiO_3$ and (b) $PbSmTiO_3$

CONCLUSIONS

The calculated equilibrium structural parameters and elastic properties of the tetragonal using the LDA-CAPZ functional are in a good agreement with the results reported in the experiment $PbLaTiO_3$ and GGA-PBEsol for $PbSmTiO_3$. Thus, this work provided an accurate structural optimization for new tetragonals $PbLaTiO_3$ and $PbSmTiO_3$ using LDA-CAPZ and GGA-PBEsol functional. We also successfully reported the relation between electronic and optical properties of tetragonal $PbLaTiO_3$ and $PbSmTiO_3$ which will provide theoretical basis that can be used by other scholars as reference in synthesizing in order to enhance the performance of $PbTiO_3$ ferroelectric systems.

ACKNOWLEDGEMENTS

The authors would like to acknowledge the Institute of Science (IOS), UiTM Malaysia for the facilities and support provided during the completion of this research. The authors also thank the Ministry of Education, Malaysia for the financial support with RAGS grantt.

REFERENCES

[1]. K. Sutjarittangtham, N. Tawichai, U. Intatha, S. Eitssayeam, K. Pengpat, G. Rujijanagul, and T. Tunkasiri, *AIP Conf. Proc.* **1151** 174–177
[2]. B. Noheda, J. Gonzalo, L. Cross, R. Guo, S.-E. Park, D. Cox, and G. Shirane, *Phys. Rev. B*, **61** (13) 8687–8695 (2000)
[3]. M. Gröting and K. Albe, *J. Solid State Chem.*, **213** 138–144 (2014)
[4]. Y. X. Wang, M. Arai, T. Sasaki, C. L. Wang, and W. L. Zhong, *Surf. Sci.*, **585** (1–2) 75–84 (2005)
[5]. M. F. M. Taib, M. K. Yaakob, O. H. Hassan, and M. Z. a. Yahya, *Integr. Ferroelectr.*, 142 (1) 119–127 (2013)
[6]. M. F. M. Taib, M. K. Yaakob, O. H. Hassan, A. Chandra, A. K. Arof, and M. Z. A. Yahya, *Ceram. Int.*, **39** S297–S300 (2013)
[7]. R. Rai, S. Sharma, N. C. Soni, and R. N. P. Choudhary, *Phys. B Condens. Matter*, 382 (1–2) 252–256 (2006)
[8]. J. Zaanen, G. Sawatzky, and J. Allen, *Phys. Rev. Lett.*, **55** (4) 418–421 (1985)
[9]. S. J. Clark, M. D. Segall, C. J. Pickard, P. J. Hasnip, M. I. J. Probert, K. Refson, and M. C. Payne, *Zeitschrift für Kristallographie*, **220** 567–570 (2005)
[10]. A. Janotti and C. G. Van de Walle, *Adv. Calc. Defects Mater. Electron. Struct. Methods*, **804** (4) 155–164 (2011)
[11]. M. K. Yaakob, M. F. M. Taib, M. S. M. Deni, and M. Z. a. Yahya, *Integr. Ferroelectr.*, **155** (1) 134–142 (2014)
[12]. A. Bouhemadou, R. Khenata, M. Chegaar, and S. Maabed, *Phys. Lett. A*, **371**, (4) 337–343 (2007)
[13]. A. K. Kalyani, L. K. V, A. R. James, A. Fitch, and R. Ranjan, *J. Phys. Condens. Matter*, **27** (7) 072201 (2015)
[14]. J. Baedi, M. R. Benam, and M. Majidiyan, *Phys. Scr.*, **81** (3) 035701 (2010)